Analytical studies of fronts, colonies, and patterns: Combination of the Allee effect and nonlocal competition interactions

M. G. Clerc,[1,2] D. Escaff,[2,3] and V. M. Kenkre[2]

[1]*Departamento de Física, Facultad de Ciencias Físicas y Matemáticas, Universidad de Chile, Casilla 487-3, Santiago, Chile*

[2]*Consortium of the Americas for Interdisciplinary Science and Department of Physics and Astronomy, University of New Mexico, Albuquerque, New Mexico 87131, USA*

[3]*Complex Systems Group, Facultad de Ingeniería y Ciencias Aplicadas, Universidad de los Andes, Av. San Carlos de Apoquindo 2200, Santiago, Chile*

(Received 19 July 2010; published 30 September 2010)

We present an analytic study of traveling fronts, localized colonies, and extended patterns arising from a reaction-diffusion equation which incorporates simultaneously two features: the well-known Allee effect and spatially nonlocal competition interactions. The former is an essential ingredient of most systems in population dynamics and involves extinction at low densities, growth at higher densities, and saturation at still higher densities. The latter feature is also highly relevant, particularly to biological systems, and goes beyond the unrealistic assumption of zero-range interactions. We show via exact analytic methods that the combination of the two features yields a rich diversity of phenomena and permits an understanding of a variety of issues including spontaneous appearance of colonies.

DOI: 10.1103/PhysRevE.82.036210 PACS number(s): 89.75.Kd, 87.23.Cc, 87.18.Hf, 82.40.Ck

I. INTRODUCTION

Among complex aspects of the spatiotemporal evolution of a variety of systems, physical, chemical, biological, and ecological are front propagation, spiral waves, localized structures, and a variety of self-organized patterns [1–5]. One way to describe the complexity of these entities is to analyze the dynamics of one or more relevant density fields as continuous variables of space and time and to find solutions of the resulting so-called "reaction-diffusion" equations. These equations are deterministic nonlinear partial differential equations sometimes possessing additional features such as nonlocality in space. Their focus is the description of the density fields of the interacting individual objects. The interactions among the individuals and with the environment are described by the reaction term (nonlinearity) while the transport is typically modeled by the diffusive term, the interplay of the nonlinearity, and the diffusion being responsible for the richness of the behavior exhibited. In the simplest cases, interactions with the environment are normally assumed to occur in the immediate outskirts of the individual, with a resulting spatially local representation. Needless to say, there are systems in which this assumption is not realistic. There may be an interaction-induced modification of the environment around the individual and the elemental reaction term may therefore be more appropriately spatially nonlocal. Pattern formation resulting in such a situation which calls for the use of an integral kernel and makes the mathematical object of analysis an *integrodifferential* equation is the general interest of the present investigation. Analysis of this general topic may be found in Refs. [1,5–18] in the context of a variety of subjects including the propagation of infectious diseases, firing of cells, and vegetation patterns.

We take as our point of departure the viewpoint developed several years ago by one of the present co-authors and his collaborators [6–8] on the basis of a nonlocal generalization of a Fisher equation which incorporates a logistic reaction-diffusion term. A couple of years ago the present authors reported [14] initial studies of the application of that viewpoint to systems in which a richer reaction-diffusion term than the logistic is operative. The present paper offers *a completely analytic* study along that direction combining the features of interaction over finite distances with richer nonlinearities that incorporate the so-called Allee effect [19–21] which will be discussed below. We find a number of useful results. The noteworthy feature of the results is that most of them are exact rather than numerically obtained [1,6–12]. This ensures their correctness for the model considered and allows comparison with numerically found results in other models where such analytic calculations are not possible.

The paper is set out as follows. Our starting point and findings are described briefly in Sec. II. The quantitative formulation of the equations and the form of the influence functions, representative of the nonlocal competition interaction, are in Sec. III. Our analytic approach including the detail of what feature of the chosen influence function allows us to obtain exact solutions is detailed in Sec. IV. Structures that emerge, including fronts, colonies, and patterns, are discussed in Sec. V, the complete phase diagram derived thus analytically is displayed in Sec. VI along with a comparison to that obtained numerically for other influence functions, and the concluding remarks are presented in Sec. VII.

II. OUR STARTING POINT AND FINDINGS

Our analysis takes as input the twin features of interaction at a distance and the Allee effect [19–21]. The latter means that the reaction term or nonlinearity in our system is such that the population suffers extinction if it starts out at sufficiently low levels of population density, that its growth overwhelms this tendency to extinction if the density exceeds certain levels, and that at sufficiently high levels a saturation effect sets in counteracting a Malthusian explosion. The simplest model is described by what we have called the Nagumo

equation in the previous work [7,22,23]: the nonlinearity is a polynomial of order 3 in the population density (unlike of order 2 which is true of the Fisher equation), the extinction tendency at low population being linear in the density as it would be by natural death, the growth being bilinear as it might be if reproduction is sexual, and a competition term which is cubic in the density.

Our focus is on the interplay of the Allee effect represented by such a cubic polynomial nonlinearity (and the ever present diffusion process) with a spatially nonlocal competition interaction. The latter means that the cubic competition term is proportional to the product of the densities not necessarily at the same location but *at different locations* as well; the strength of the competition is described by an *influence function* characterized by a given width and shape [6]. We restrict our analysis here to two specific influence functions: the step function and the exponential. The first, while formally simple, requires numerical analysis. The second, the primary focus of this paper, allows essentially all calculations to be carried out analytically and is a mod exponential. The explicit equations are given in Sec. III.

We are able to explore traveling fronts, stationary states, localized structures including those that may be termed colonies, and infinite size patterns all emerging from the interplay of the two features we study. Colonies and the patterns states are self-organized steady states. Specific results we obtain include the following: (a) information about the stability of the homogeneous state with zero, partial, and full populations; (b) appearance and disappearance of self-organized structures (patterns) as the spatial extent of the range of the (nonlocal) competition interaction is changed; (c) appearance of traveling front solutions and information about their speed; (d) appearance of stable isolated solutions (that we have previously termed horn solutions, which colonies state); (e) analytical determination and characterization of the critical point in parameter space where colonies make their appearance; (f) emergence of localized patterns as consequence of the interplay of patterns and homogeneous states; and (g) exact (analytical) determination of the phase diagram and comparison with numerical simulations in earlier literature.

III. FORM OF THE EQUATION OF EVOLUTION AND INFLUENCE FUNCTION

Our systems consist of individuals making up a field (e.g., atoms or molecules in physical systems and bacteria or animals in biological systems) of density $U(X,T)$, where X and T are space (considered one dimension for simplicity) and time, respectively, moving diffusively with diffusion constant D and nonlinearities characterized by coefficients A, B, and C such that, without nonlocal competition effects, the dynamics would obey

$$\partial_T U = D\partial_{XX} U - AU + BU^2 - CU^3. \tag{1}$$

The nonlinear reaction terms describe natural death at rate A, growth that might be reproductive controlled by B, and a saturation term that is proportional to C. Let the roots of the nonlinear reaction polynomial be 0, $U_{unst} \equiv (B + \sqrt{B^2-4AC})/2C$ and $U_{max} \equiv (B - \sqrt{B^2-4AC})/2C$ in respective order of magnitude, the suffixes denoting the unstable root and the maximum (saturation) value of U, respectively.

We now introduce the parameter $\alpha \equiv -(1-B/2AC) + \sqrt{(1-B/2AC)^2+1}$ and dimensionless variables for space, $x = \sqrt{A/\alpha D}X$, for time $t = TA/\alpha$, and the population field, $U = \sqrt{A/C\alpha}u$, incorporate nonlocality in the competition (cubic) term, and write the starting equation of our analysis as

$$\partial_t u = \partial_{xx} u - \alpha u + (\alpha+1)u^2 - u\int_\Omega u^2(x',t) f_\sigma(x-x')dx', \tag{2}$$

where u outside the integral denotes $u(x,t)$. We point out that the nonlocality in the competition interaction can generally appear in one of the several ways although we have chosen the form of the term as the integral of $-u(x,t)u^2(x',t)f_\sigma(x-x')$. Our choice makes the model variational and allows an easier path in the calculations. Other choices are $-u^2(x,t)u(x',t)f_\sigma(x-x')$ which leads to a nonvariational system and $-u(x,t)u(x',t)u(x'',t)f_\sigma(x-x')f_\sigma(x'-x'')$ which requires two integrations. We intend to treat these additional choices in a future publication. Note that f_σ is normalized, i.e., its integral is 1, and that Ω represents all the space under consideration; for instance, if the system is infinite $\Omega = (-\infty,\infty)$.

Our starting Eq. (2) is characterized generally by the shape of the influence function and specifically by its range which we will denote below by σ. We have taken the f_σ to be a function of the difference $(x-x')$ to restrict consideration to translational invariant systems, although it is certainly possible to consider nondifference kernels. Our starting point (2) is additionally characterized by the single parameter α. This parameter α, which lies between 0 and 1 and which we call the "adversity," is crucial to the analysis as we will see below. Indeed, the phase diagram of the system will be naturally given in α-σ space.

Earlier work on this topic [1,6–8] which introduced nonlocality into the Fisher equation employed a variety of influence functions. Our present work focuses on a specific choice not studied earlier, the mod exponential function [see Fig. 1(a)], because it allows us to develop analytic procedures for investigation as we shall show below. It is given by

$$f_\sigma(z) = \frac{e^{-|z|/\sigma}}{2\sigma}, \tag{3}$$

where $z \equiv x-x'$. We will also study, for comparison purposes, the step influence function used earlier [6–8] and given by [see Fig. 1(b)]

$$f_\sigma(z) = \frac{\theta(z+\sigma)\theta(z-\sigma)}{2\sigma}. \tag{4}$$

Despite its simplicity, the step form does not allow the analytic procedures we develop for the exponential influence function. On the other hand, numerically, the step function is preferable as it involves only a finite region of space.

An important general feature of our starting Eq. (2) is that what is termed "variational" or gradient; i.e., it can be derived from a Lyapunov functional $\mathcal{F}[u]$ through

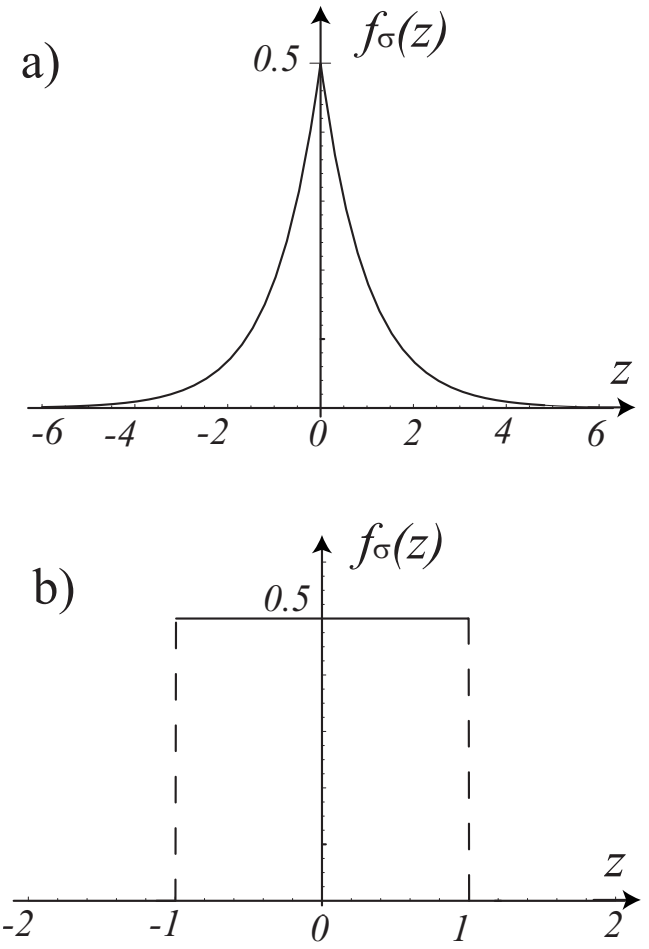

FIG. 1. The two influence functions analyzed in the present paper ($\sigma=1$): (a) exponential influence function, of primary interest to the analysis, given in Eq. (3) and (b) step influence function, treated in earlier work, given in Eq. (4).

$$\partial_t u = -\frac{\delta \mathcal{F}[u]}{\delta u},$$

where the Lyapunov functional is explicitly given as

$$\mathcal{F}[u] = \int_\Omega \left\{ \frac{1}{2}(\partial_x u)^2 + \frac{\alpha}{2}u^2 - \frac{(\alpha+1)}{3}u^3 \right\} dx + \frac{1}{4}\int_\Omega \int_\Omega u^2 u'^2 f_\sigma(x,x')dxdx'. \quad (5)$$

Hence, the dynamical behavior of our system is of relaxation type, that is, the evolution of dynamical system (2) always proceeds to minimize of $\mathcal{F}$, the stationary states being local minima of $\mathcal{F}[u]$.

It is clear that our system has three homogeneous equilibrium states: $u(x,t)=0$, $u(x,t)=1$, and $u(x,t)=\alpha$, which we will call the unpopulated, populated, and partially populated state for obvious reasons, respectively. For small σ, the first two constitute stable fixed points while $\{\alpha\}$ represents an unstable fixed point. The adversity α determines the global stability of the attractors. Evaluating the Lyapunov functional in the stable equilibria states, one obtains

$$\mathcal{F}[u=0]=0; \quad \mathcal{F}[u=1]=\left(\int_\Omega dx/6\right)(\alpha-1/2).$$

As is well known [24], the equality of the two values of the Lyapunov functional marks the so-called Maxwell point. For our system it is given by $\alpha=\alpha_M \equiv 1/2$. We see that the Maxwell point is independent of the influence function.

IV. ANALYTIC INVESTIGATION FOR THE MOD EXPONENTIAL INFLUENCE FUNCTION

As is well known, necessary (but not sufficient) conditions for the appearance of nonhomogeneous solutions may be obtained by the methods of linear stability. We first apply this well-known method to our problem along the lines of our previous calculations for the Fisher system [8], making it clear however how our choice in the present paper allows explicit analytic calculations of the relevant separatrix curve. We then also show how the construction of a fictitious four-dimensional associated system allows exact analysis.

A. Spectrum and separatrix

If we expand $u=u_0+v$ around the three states of our system mentioned above, the value of u in the homogeneous state being u_0, substitute the expansion in Eq. (2), and neglect powers of v higher than 1 by considering v as a small perturbation, we can write out the equations of linear dynamics and from them obtain the spectrum near each homogeneous state—set of eigenvalues that characterize linear operator. We do this for all three homogeneous states. The linear dynamics close to $u_0=0$, the unpopulated state, is

$$\partial_t v = \partial_{xx} v - \alpha v,$$

while close to $u_0=1$, the fully populated state, it is

$$\partial_t v = \partial_{xx} v + (\alpha+1)v - 2\int_\Omega v(z) f_\sigma(z) dz.$$

Both these are stable homogeneous states, for small σ, and therefore important to consider. For completeness we also mention that close to $u_0=\alpha$, the partially populated (unstable) state, the linear dynamics is given by

$$\partial_t v = \partial_{xx} v + (\alpha+\alpha^2)v - 2\alpha^2\int_\Omega v(z) f_\sigma(z) dz.$$

In each case, to obtain the spectrum, we Fourier transform $v(x,t)$. Equivalently, we take $v(x,t)$ to be proportional to $e^{\lambda t+ikx}$ and substitute it in the time evolution equations above to obtain the relation between the wave number k and λ. This relation is the desired spectrum.

We find, in turn, that the spectra are

$$\lambda(k) = -k^2 - \alpha$$

near the unpopulated state,

$$\lambda(k) = -k^2 + (\alpha+1) - 2\hat{f}_\sigma(k)$$

near the fully populated state, and

$$\lambda(k) = -k^2 + (\alpha + \alpha^2) - 2\alpha^2 \hat{f}_\sigma(k)$$

near the partially populated state. Important to note are two points. The first is that the spectrum is controlled, as observed earlier in Refs. [7–9] by the influence function through its Fourier transform $\hat{f}_\sigma(k) = \int_\Omega \cos(z) f_\sigma(z) dz$, we restrict our consideration to even influence functions only for simplicity. The second point is that, unlike for the Fisher equation (characterized by a logistic nonlinearity) analyzed in Refs. [7,8], the present Nagumo equation analysis provides a *further control* over the stability through the constant terms in the spectrum which are proportional to the adversity α and its square. This changes the situation profoundly from that analyzed in Refs. [7,8] and allows for patterns and other structures to emerge more easily from our system.

We can deduce immediately that the unpopulated state is always a stable state in that a perturbation from it always decays and that it is diffusive and of the relaxation type; that is, if one considers initially a positive perturbation, this perturbation remains always positive and smaller than its earlier value [1], eventually going to zero. The behavior near the populated states depends on the form of the (Fourier transform of the) influence function. For exponential influence function (3), the Fourier transform is

$$\hat{f}_\sigma(k) = \frac{1}{1 + (k\sigma)^2},$$

while for step influence function (4) it is [8]

$$\hat{f}_\sigma(k) = \frac{\sin(k\sigma)}{k\sigma}.$$

The dynamics close to $u=1$ shows that spatial instability can set in when the system parameters are changed. This can be seen in Fig. 2: some λ values become positive and so the respective Fourier modes or eigenvectors can increase exponentially with time. In order to obtain the zone in the parameters space $\{\alpha, \sigma\}$ where the fully populated state is stable or unstable, we must solve the equations (bifurcation condition)

$$\lambda(k_c) = 0 \quad \text{and} \quad d\lambda(k_c)/dk = 0.$$

From these conditions, we obtain the separatrix curve $\sigma_c = S(\alpha)$. If σ is larger (smaller) than $S(\alpha)$, then the fully populated state is spatially unstable (stable). For exponential influence function (3), we have the explicit expression

$$\sigma_c = S(\alpha) = \frac{\sqrt{2} + \sqrt{1-\alpha}}{1+\alpha}. \tag{6}$$

For step influence function (4) the curve $S(\alpha)$ has to be calculated numerically. In Fig. 3, the curve $S(\alpha)$ is represented by the solid line for the exponential and step influence function. Our numerical solution of the model uses an explicit Runge-Kutta order 4 scheme in one-dimensional line space grids of size 256 or 1000. On the line $S(\alpha)$, the homogenous state $u=1$ suffers a spatial instability given rise to spatial periodic solution, *population pattern state.* This self-organization response, the pattern population state, gives to the population a better capacity to deal with the adversity imposing by the environment characterized by the range of the influence function σ. Figure 4 shows the typical pattern observed in model (2).[1]

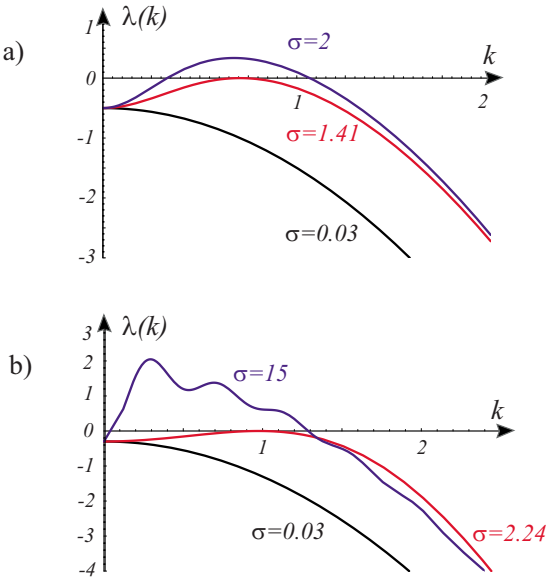

FIG. 2. (Color online) Spectrum: linear growth rate λ as a function of the wave number k of the fully populated state $u(x,t)=1$. (a) Spectrum for exponential influence function with $\alpha=0.5$ and (b) spectrum for the step influence function with $\alpha=0.7$.

B. Construction of a four-dimensional associated system for exact calculations

To characterize the stationary bifurcation of model (2) for the mod exponential influence function, we consider the stationary system $u(x,t)=u(x)$,

$$0 = \partial_{xx} u - \alpha u + (\alpha+1)u^2 - u \int_\Omega u'^2 f_\sigma(x,x') dx'. \tag{7}$$

Notice that by reinterpreting x as time, Eq. (7) can be looked upon as a part of a second-order (in x) equation of motion for a dynamical system characterized by two variables and their x derivatives. One of the variables is u. The other is a quantity $w(x)$ that satisfies

$$\left(\partial_{xx} - \frac{1}{\sigma^2}\right) w = -\frac{u^2}{\sigma^2}. \tag{8}$$

Moreover, the exponential influence function complies with

$$\left(\partial_{xx} - \frac{1}{\sigma^2}\right) f_\sigma(x - x') = -\frac{\delta(x-x')}{\sigma^2}. \tag{9}$$

Hence, f_σ is the Green's function of the operator $(\partial_{xx} - \sigma^{-2})$, then

$$w = \int_{-\infty}^{\infty} u'^2 f_\sigma(x,x') dx'.$$

[1]The simulation software *DimX* developed by P. Coullet and collaborators at INLN in France has been used for all the numerical simulations.

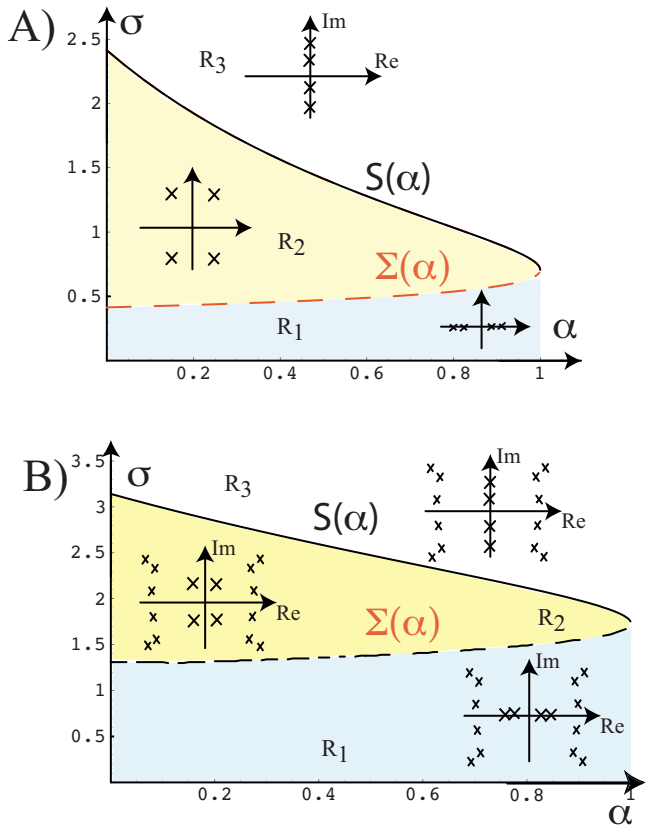

FIG. 3. (Color online) Bifurcation diagram of variational nonlocal Nagumo model. (a) Bifurcation diagram of the exponential influence function and (b) bifurcation diagram of the step influence function. The $S(\alpha)$ curve is the bifurcation line where the fully populated state exhibits a spatial instability, $\Sigma(\alpha)$ curve is the bifurcation line where the front solution, between the unpopulated and fully populated states, loses the monotonic profile, and the inset figures are the spectrum of spatial dynamics system in the respective zone.

Hence, we can rewrite the spatial equation [Eq. (7)] in the following form (spatial dynamic system):

$$\partial_{xx}u = \alpha u - (\alpha+1)u^2 + uw,$$

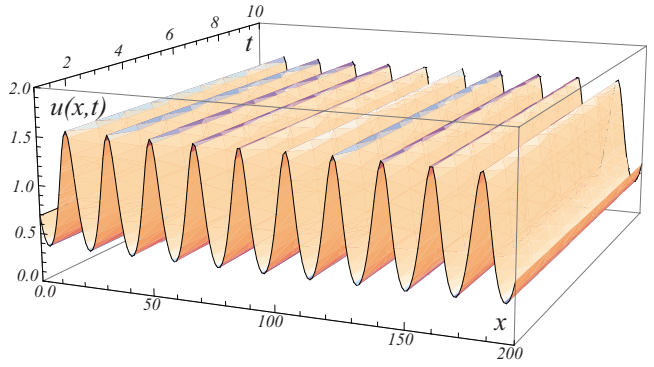

FIG. 4. (Color online) Spatiotemporal diagram of the pattern population state, observed in variational nonlocal Nagumo model for the exponential influence function, $\alpha=0.34$, $\sigma=1.8$, and system size=200.

$$\partial_{xx}w = \frac{(w-u^2)}{\sigma^2}. \tag{10}$$

The fixed points of above dynamical system are

$$(u,\partial_x u,w,\partial_x w) = \{(0,0,0,0);(\alpha,0,\alpha^2,0);(1,0,1,0)\},$$

which correspond to the uniform solution of variational nonlocal Nagumo model (2). To characterize these fixed points, we must linearize the dynamics around them.

Unpopulated state. The spatial dynamics close to this state are characterized by the operator

$$L_0 = \begin{pmatrix} 0 & 1 & 0 & 0 \\ \alpha & 0 & 0 & 0 \\ 0 & 0 & 0 & -2/\sigma^2 \\ 0 & 0 & -1/2 & 0 \end{pmatrix},$$

with the eigenvalues $\{\sqrt{\alpha},-\sqrt{\alpha},1/\sigma,-1/\sigma\}$, which are pure real numbers. Hence, this fixed point is always a hyperbolic fixed point.

Fully populated state. The spatial dynamics around the fully populated state are characterized by the linear operator

$$L_1 = \begin{pmatrix} 0 & 1 & 0 & 0 \\ -(1+\alpha) & 0 & 1 & 0 \\ 0 & 0 & 0 & -2/\sigma^2 \\ 1 & 0 & -1/2 & 0 \end{pmatrix}$$

with the eigenvalues $\{(a+b)^{1/2},-(a+b)^{1/2},(a-b)^{1/2},-(a-b)^{1/2}\}$, where

$$a \equiv \frac{1}{2\sigma^2}[1-(1+\alpha)\sigma^2],$$

$$b \equiv \frac{1}{2\sigma^2}\sqrt{[1-(1+\alpha)\sigma^2]^2 - 4(1-\alpha)\sigma^2}. \tag{11}$$

The spectrum presents three possibilities according to whether the four eigenvalues are (i) pure real, (ii) complex, that is, with a nonvanishing real and imaginary parts, and (iii) pure imaginary. Correspondingly, we divide the parameter space in three zones $R_1=\{0<\sigma<\Sigma(\alpha)\}$, $R_2=\{\Sigma(\alpha)<\sigma<S(\alpha)\}$, and $R_3=\{S(\alpha)<\sigma\}$, where $0<\alpha<1$.

The curve

$$\Sigma(\alpha) = \frac{\sqrt{2}-\sqrt{1-\alpha}}{1+\alpha}$$

corresponds, in parameter space, to the bifurcation when the eigenvalues are pure real with multiplicity two. This means that below the Σ curve the eigenvalues lie on the real axis while above this curve they are complex with nonvanishing imaginary part [cf. Fig. 3(a)]. The S curve coincides with condition (6) and this curve corresponds, in the parameter space, to the bifurcation when the eigenvalues are pure imaginary with multiplicity two, that is, above the S curve the eigenvalues are pure imaginary and below this curve the eigenvalues are complex number with non-null real part.

In region R_1, the fully populated state is a hyperbolic fixed point with all its eigenvalues pure real numbers. The

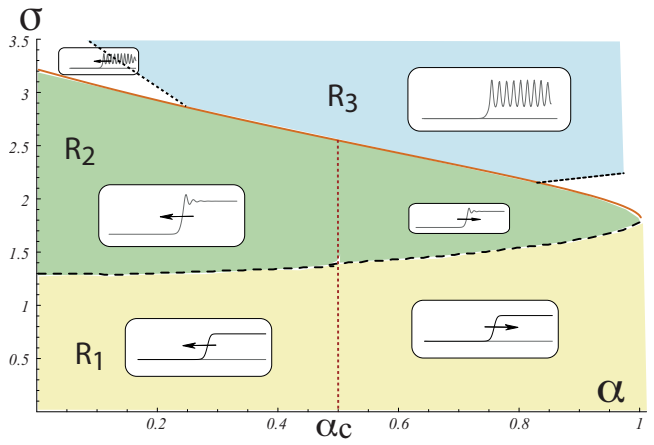

FIG. 5. (Color online) Bifurcation diagram of the front solutions for the variational nonlocal Nagumo model. In the R_1 region, the front solutions are monotonic functions and are motionless in the Maxwell manifold ($\alpha_c=1/2$). In the R_2 region, the front solutions between the fully populated and unpopulated states exhibit spatial damped oscillations and are motionless in the Maxwell manifold. In the R_3 region, the system exhibits coexistence between the pattern population and unpopulated states; model (2) has front solutions between these states.

system exhibits the same qualitative behavior as in the extreme local limit $\sigma \to 0$. Hence, we have called this parameter region the *Nagumo zone*. In region R_2, the fully populated state is also hyperbolic fixed point, but now its eigenvalues have nonvanishing imaginary part. Then, the stationary trajectories that link this uniform state with other state exhibit a damped spatial oscillations close to this fixed point. In region R_3, the eigenvalues of the fully populated state become pure imaginary; this event coincides with the spatial instability of the fully populated state in variational nonlocal Nagumo model (2). That is, the hyperbolic fixed points (1,0,1,0) becomes center; then, this solution is surrounded by spatial periodical solutions. One of these orbits is selected to be the stable pattern.

On the bases of central manifold theorem [25], one can show that the spatial dynamical system related to the step influence function is quite similar to those related to the exponential influence function. In Fig. 3(b), the different zones obtain numerically for the step influence function.

C. Front between the unpopulated and the fully populated states

An extended system that shows coexistence of stationary states generically can exhibit solutions that connect these states [1,4]. The energy of each state being different, the more favorable state invades the less favorable one. This phenomenon is well known as front propagation [1,4,26]. From the point of view of dynamical system theory, this type of solution corresponds to a heteroclinic solution [27]. A front solution connecting the unpopulated and the fully populated states is motionless at the Maxwell point because both states have the same energy [24]. In Fig. 5 the inset images illustrate the front solutions observed in nonlocal variational Nagumo model (2) in the respective regions. The Maxwell point is represented by a vertical dashed line in parameter space, which crosses the regions R_1 and R_2.

To study the dynamics of front propagation, we will use the standard strategy of considering the parameter region where the front is stationary. Using the condition of persistence of the front solution, one can deduce the front speed law [27]. To study the dynamics of front propagation around the Maxwell point, we denote the motionless front solution by $u_F^{\pm}(x-P)$, where the upper index + (−) means a spatial connection of the fully populated (unpopulated) state from $-\infty$ to the unpopulated (fully populated) one at ∞. Here, P is a parameter that characterizes the position of the front core, defined as the spatial location where the spatial derivative of front solution is maximum. Considering the adversity $\alpha = \alpha_M + \eta$ (where η is infinitesimal), the front solution propagates in order to minimize the Lyapunov function $\mathcal{F}$. To account for this, we consider the ansatz

$$u(x,t) = u_F^{\pm}[x - P(t)] + \phi_1(x,P) + \text{higher order terms},$$

where $P(t)$ is a slow variable and $\phi_1(x,P)$ is a small correction function $[\phi_1 \sim \dot{P} \sim \eta \ll \mathcal{O}(1)]$. Introducing this approach in model (2) and linearizing with respect to ϕ_1, we obtain

$$\mathcal{L}_{1/2}(u_F^{\pm})\phi_1 = \eta(1-u_F^{\pm})u_F^{\pm} - (\partial_x u_F^{\pm})\dot{P}, \tag{12}$$

where

$$\mathcal{L}_{\alpha}(u_F^{\pm})\phi_1 \equiv \partial_{xx}\phi_1 - \alpha\phi_1 + 2(\alpha+1)u_F^{\pm}\phi_1 - 2u_F^{\pm}\int_{\Omega} f_{\sigma}(x,x')u_F^{\pm}(x')\phi_1(x')dx' - \phi_1\int_{\Omega} f_{\sigma}(x,x')u_F^{\pm}(x')^2 dx'. \tag{13}$$

Introducing the inner product $\langle f|g\rangle = \int_{\Omega} f(x)g(x)dx$, one can show that $\partial_x u_F^{\pm}$ is an element of the kernel of the adjoint operator $\mathcal{L}_{1/2}(u_F^{\pm})$. Hence, to solve Eq. (12), we must impose the solvability condition or the Fredholm alternative [4]. We multiply the right-hand side of Eq. (12) by $\partial_x u_F^{\pm}$ and integrate in the entire domain. We then obtain the front speed law

$$\dot{P} = \mp \frac{\eta}{6\int_{\Omega}(\partial_x u_F^{\pm})^2 dx} \equiv c_{\pm}, \tag{14}$$

where the dot signifies time derivative and $c_{\pm}$ is the front speed proportional to $\eta = \alpha - \alpha_M$. Figure 6 illustrates the front propagation observed in the region R_2. When η is negative (positive), the fully populated state is less (more) favored than the unpopulated state and the front propagates from the unpopulated (fully populated) to fully populated (unpopulated) state in order to minimize the Lyapunov function $\mathcal{F}$.

The previous analytical analysis is valid close to the Maxwell point. Numerically, the same qualitative dynamical behavior is observed far from the Maxwell point. Consequently, the system tries to minimize Lyapunov functional (5). Hence, fronts propagate with the same prescription, that is, with a constant speed and the most favored state invades

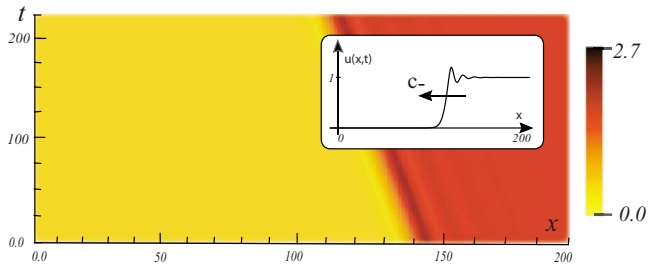

FIG. 6. (Color online) Spatiotemporal evolution of the population density $u(x,t)$ for model (2), in the case of step influence function, α=0.4, σ=2.475, and system size=200; time runs upward. The intensity of the gray scale is proportional to population density. The inset figure is the initial population density profile.

the less favored one. The derivation of an explicit expression of the front speed far form the Maxwell point is generically a rather complex problem.

Figure 5 shows the bifurcation diagram for the different front solutions observed in model (2). In the region R_1, front solutions exhibited by the variational nonlocal Nagumo model are quite similar to those observed in the Nagumo model. In the region R_2, front solutions exhibit spatially damped oscillations close to the Maxwell curve (cf. inset of Fig. 3). This spatial damped oscillations are a consequence of the fact that the eigenvalues of spatial dynamical system—related to the fully populated state—have non-null imaginary part (cf. Fig. 2). The frequency of these spatial oscillations is the imaginary part of these eigenvalues.

V. PATTERNS AND COLONIES

On the curve $S(\alpha)$, the fully populated state undergoes a spatial instability, which gives rise a periodic solution. We call this the pattern state. Numerically, we observe that above this curve the system has pattern states, which show different amplitudes depending on the value of adversity parameter. In order to understand the mechanism of emergence of these patterns, we carry out a weakly nonlinear study near the instability region.

A. Universal description close to $S(\alpha)$

Close to the spatial bifurcation curve $\sigma_c = S(\alpha)$, we can use the standard weakly nonlinear analysis of amplitude equations [3,4,28]. We use the ansatz

$$u(x,t) = 1 + A(t)\cos(k_c x) + \text{higher order terms},$$

where A is the pattern amplitude and k_c is the critical wave number. Introducing the above ansatz in model (2) and after straightforward calculations based on the theory of normal forms [28], we obtain the following equation for the amplitude:

$$\partial_t A = \varepsilon A - \beta A^3, \tag{15}$$

where

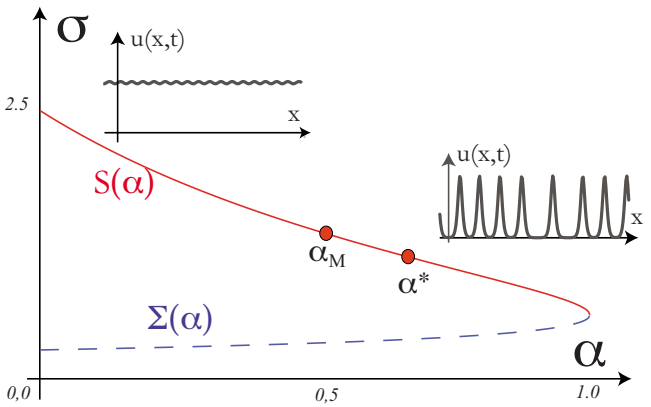

FIG. 7. (Color online) Schematic representation of bifurcation diagram of the variational nonlocal Nagumo model (2) for the exponential influence function. α_M and α^* are the Maxwell point and the point where the spatial instability changes from supercritical to subcritical, respectively. In the inset figures, we see the pattern observed above the $S(\alpha)$ curve before and after the α^* point.

$$\beta = \left\{ \frac{(1-k_c^2)^2}{\alpha - 1} + \frac{[\hat{f}_\sigma(2k_c) - k_c^2]^2}{2[-4k_c^2 + (\alpha+1) - 2\hat{f}_\sigma(2k_c)]} + \frac{1}{4}[\hat{f}_\sigma(2k_c) + 2] \right\}$$

and ε is the bifurcation parameter that is proportional to $(\sigma - \sigma_c)$. The above amplitude equation describes a stationary pitchfork bifurcation [29]. When ε is negative, the fully populated state is stable. For positive ε, the solution is unstable and the system exhibits pattern formation with the amplitude going as $\sqrt{\varepsilon/\beta}$ for positive β. Variational nonlocal Nagumo model (2) can be approached with the help of Eq. (15) when the amplitude and parameters satisfy the scaling $\partial_t \sim \varepsilon$, $A \sim \varepsilon^{1/2}$, $\beta \sim O(1)$, and $\varepsilon \ll 1$. Indeed, while the bifurcation parameter is small, one can neglect the higher order terms that amend Eq. (15). For positive (negative) β, the bifurcation is supercritical (subcritical) [29]. Then, when β is zero, the system shows a transition between supercritical and subcritical bifurcations.

For both influence functions, numerically we have computed the point in the parameter space where the coefficient $\beta[S(\alpha^*), \alpha^*]$ is equal to zero, i.e., the transition point, where $\alpha^* \cong 0.742$ or $\alpha^* \cong 0.657$ for the step or exponential influence functions, respectively (cf. Fig. 7). Hence, on the $S(\alpha)$ curve for $\alpha < \alpha^*$, the fully populated state becomes unstable and the bifurcation is supercritical. Numerically, we observe emergence of patterns around the fully populated state with small amplitude of the order $\sqrt{\varepsilon}$ (cf. inset of Fig. 7). For $\alpha > \alpha^*$, the spatial bifurcation is subcritical, that is, we have an unstable periodical solution with finite amplitude surfaces for $\sigma > S(\alpha^*)$ (cf. Fig. 7). In general, dynamical behavior cannot be described in terms of weakly nonlinear analysis.

B. Front between the unpopulated states and the pattern state

In the R_3 region, model (2) exhibits coexistence between the unpopulated state and pattern state. Numerically, we ob-

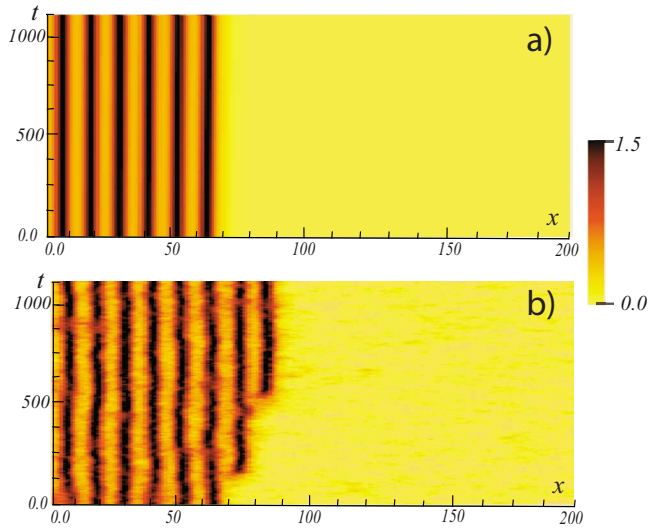

FIG. 8. (Color online) Spatiotemporal evolution of the population density $u(x,t)$ for model (2), with time running up, α=0.33, σ=2.7, (a) without noise, and (b) plus additive noise. The gray scale is proportional to the population density.

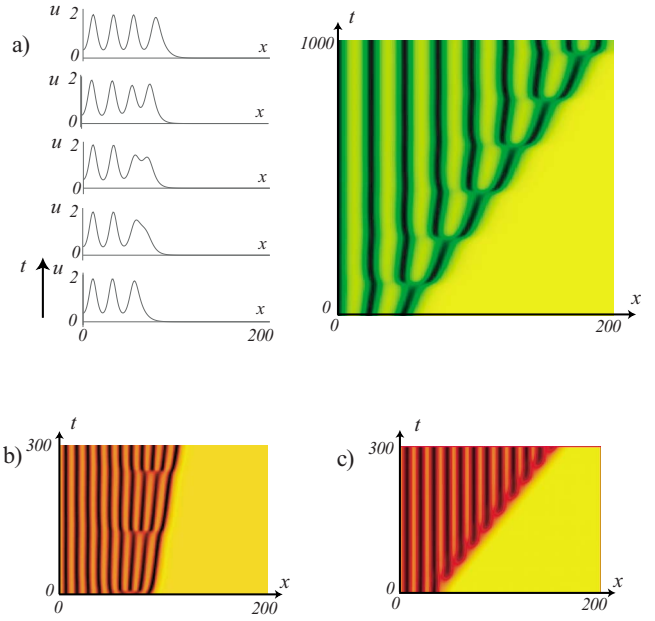

FIG. 9. (Color online) Front propagation, spatiotemporal evolution of the population density $u(x,t)$ for model (2), with time running up (a) α=0.08 and σ=2.4 for exponential influence function, (b) α=0.31 and σ=2.9 for step influence function, and (c) α=0.054 and σ=3.32 for step influence function.

serve front solutions connecting these two states. A front solution that links a uniform state with an spatial periodic one is motionless in a region of the parameter space [4,30]. This phenomenon is called *locking or pinning* and the region of the parameter space where the front is motionless is called the *pinning range*. The origin of this phenomenon is related to the fact that the spatial periodic solutions break the translational symmetry and the system now is only invariant under discrete spatial translation. Hence, the front cannot move forward or backward because the front must cross a periodical nucleation barrier [31]. These motionless front solutions do not represent the global minimum of Lyapunov functional (5). However, they do represent a local minimum. Hence, in the pinning region, the population can spread only if one adds energy to the system. For instance, if we consider the effect of additive noise, the fully populated state can invade the unpopulated one. This phenomenon is known as noise-induced front propagation [31]. Figure 8 depicts the spread of population as a result of the inclusion of additive noise in the variational nonlocal Nagumo model.

It is important to note that, outside the pinning range and for small (large) adversity, the fronts propagate with an oscillatory speed and the fully populated (unpopulated) state invades the other (cf. Fig. 9). The origin of the spatial oscillation of front speed is related to the fact that the pattern state breaks the spatial translation symmetry [30]. Figure 9 illustrates the front propagation, which is related to the self-replication process exhibited in model (2) [15]. Figure 9(a) replicates the cell at the border of the interface, while Fig. 9(b) replicates the second cell nearest to the interface. In Fig. 9(c) the front propagation is more conventional, just a new cell appears at the interface.

C. Colonies

By the term "colony" we mean a stable isolated population region, that is, a state characterized by a region with high population density surrounded by low population density. From a dynamical point of view a colony arises from a homoclinic solution, that is, a solution that asymptotically connects one state (unpopulated) with itself [27]. Hence, depending on the coexistence of different extended states, one expects different types of colonies. In Sec. V C 1, we characterize the different colony type solutions exhibited by model (2). In particular, we use the front interaction to determine the emergence of colonies.

1. Localized domains in the R_2 region: Horn solutions

A simple way to understand localized population states is based on the front interaction [27] in that a localized solution is constituted by two interacting fronts. This approach is correct when the distance between the fronts is larger than the size of core (see review [27], and references therein). To study the front interaction, let us investigate what happens near the Maxwell point. We consider a solution consisting of two fronts, that is,

$$u = u_F^+\left(x - \frac{\Delta(t)}{2}\right) + u_F^-\left(x + \frac{\Delta(t)}{2}\right) - 1 + \phi_2(x,\Delta), \quad (16)$$

where $\phi_2(x,\Delta)$ is a correction function. $\Delta(t)$ stands for the distance between front cores [cf. Fig. 10(c)]. One front is affected by the other via two mechanisms: (i) the effect of the tail of a front on the other one, which corresponds to an exponential correction, and (ii) the interaction mediated by the nonlocal nonlinearity. For the step influence function or any influence function that decays asymptotically faster than an exponential function, the first mechanism will lead the interaction if the influence range is small in comparison to the distance between the front cores ($\sigma \ll \Delta$).

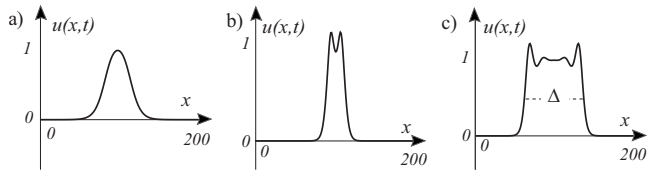

FIG. 10. Horn solutions observed in our model (2) for the exponential influence function, with system size=200 points. (a) One-bump solution with α=0.55, σ=1.3, (b) two-bump solution with α=0.49, σ=1.4, and (c) typical horn solution with α=0.5, σ=1.4. Δ is the size of the horn solution.

The exponential influence function decays exponentially. Hence, the interaction mediated by the nonlocal nonlinearity is characterized by the decay length σ. On the other hand, the influence between the fronts is characterized by the decay length $\delta \equiv 1/|\mathrm{Re}[\sqrt{a+b}]| = \rho^{-1}$, where a and b are coefficients defined in formulas (11). This decay length is the reciprocal of the real part of the eigenvalues of the fully populated state. It is easy to show that $\delta > \sigma$. Hence, the first mechanism always dominates and we can consider the following scaling:

$$\phi_1 \sim \dot{\Delta} \sim \partial_x u_F^{\pm}(\mp\Delta) \ll 1.$$

Let us focus on a spatial region around one front core, $x \sim -\Delta/2$. In this region, the front solution u_F^- takes the asymptotic form

$$u_F^-(x \sim -\infty) \simeq 1 - b_-(x),$$

where

$$b_-(x) = \begin{cases} de^{-\rho x} & \text{in the } R_1 \text{ region} \\ d\cos(\omega x)e^{-\rho x} & \text{in the } R_2 \text{ region,} \end{cases}$$

d is a positive constant that should be calculated numerically, and $\omega \equiv |\mathrm{Im}[\sqrt{a+b}]|$. Introducing ansatz (16) in variational nonlocal Nagumo model (2) at the Maxwell point and linearizing in ϕ_1, we obtain

$$\mathcal{L}_{1/2}\left[u_F^+\left(x-\frac{\Delta(t)}{2}\right)\right]\phi_2 = -\frac{\dot{\Delta}}{2}\partial_x u_F^+\left[x-\frac{\Delta(t)}{2}\right] + 3u_F^+\left(x-\frac{\Delta(t)}{2}\right)b_-\left(x+\frac{\Delta(t)}{2}\right) + 2(\mathcal{N}-1)b_-\left(x+\frac{\Delta(t)}{2}\right)$$
$$- 2u_F^+\left(x-\frac{\Delta(t)}{2}\right)\mathcal{N}\left\{u_F^+\left(x-\frac{\Delta(t)}{2}\right)b_-\left(x+\frac{\Delta(t)}{2}\right)\right\} - b_-\left(x+\frac{\Delta(t)}{2}\right)\mathcal{N}\left\{u_F^+\left(x-\frac{\Delta(t)}{2}\right)\right\}^2,$$

where the operator $\mathcal{L}_{1/2}$ is defined in expression (13) and $\mathcal{N}\psi(x) \equiv \int_\Omega f_\sigma(x,x')\psi(x')dx'$. The above linear equation for ϕ_2 has the following solvability condition (front interaction):

$$\dot{\Delta} = -Ab_-(\Delta), \tag{17}$$

where the dot signifies time derivative and A is a positive constant defined by the expression

$$A = \{\langle \partial_x u_F^+ b_- | \mathcal{N} u_F^{+2}\rangle + 2\langle u_F^+ b_- | \mathcal{N} u_F^+ \partial_x u_F^+\rangle - 3\langle \partial_x u_F^+ | u_F^+ b_-\rangle$$
$$- 2\langle b_- | (\mathcal{N}-1)\partial_x u_F^+\rangle\}/\langle \partial_x u_F^+ | \partial_x u_F^+\rangle.$$

Hence, the pair front interaction is described in Eq. (17). Outside the Maxwell point, the two-front system will be under the influence of another "force," which comes from the different of Lyapunov functional values at the uniform states. In order to depict that, we consider $\alpha = \alpha_M + \eta$, with η of order of function ϕ_1. Analogously, we obtain the following solvability condition:

$$\dot{\Delta} = -Ab_-(\Delta) + c_+, \tag{18}$$

where c_+ is defined in Eq. (14).

(a) *Front interaction in the R_1 region*. In the Nagumo zone the front interaction is always attractive,

$$\dot{\Delta} = -Je^{-\rho\Delta} + c_+, \tag{19}$$

with $J = dA > 0$ constant value. Then, the above equation has an unstable steady state at $\Delta^\dagger = \ln(c_+/J)/\rho$ close to the Maxwell point when the adversity is lower than 1/2. Hence, the system exhibits the same qualitative behavior as observed in the Nagumo model. This coincides with the fact that in this region, where the nonlocal interaction is still weak, the front connections are monotonic.

(b) *Front interaction in the R_2 region*. In this parameter region the front interaction has the form

$$\dot{\Delta} = -J\cos(\omega\Delta)e^{-\rho\Delta} + c_+. \tag{20}$$

This is the typical interaction law found for fronts with spatial damped oscillations [27]. From this equation, we deduce that the system exhibits different steady states, which correspond to localized states or colonies. The size of these solutions Δ^* satisfies the equation

$$\cos(\omega\Delta^*)\exp(-\rho\Delta^*) = -c_+/J. \tag{21}$$

We have termed these steady states as *horn solutions* [14]. Figure 10 shows typical horn solutions observed in model (2). Their lengths are approximate multiples of the shortest localized state length, which is related to the characteristic length ω of the spatially damped oscillations.

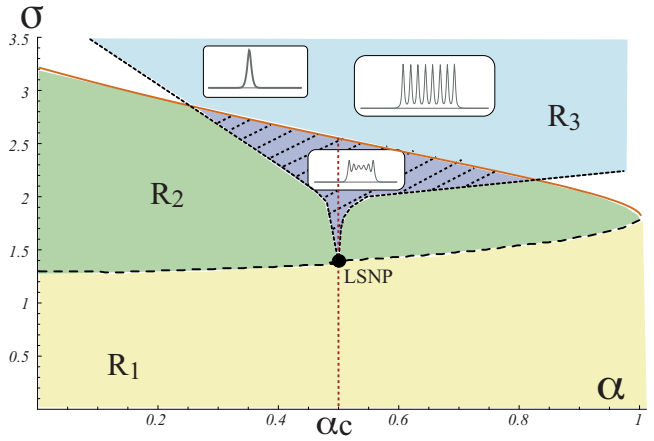

FIG. 11. (Color online) Bifurcation diagram of the localized solutions for the variational nonlocal Nagumo model. The family of horn solution appears from the codimension two-point LSNP. On R_3 zone, close to the gray zone the system exhibits localized patterns.

The point in the parameter space where the horn solutions appear is determined by the intersection between the Maxwell manifold and the Σ curve,

$$(\alpha,\sigma) = (1/2, \Sigma(1/2)).$$

We term this point the *localized structure nascent point* (LSNP). Figure 11 shows this point in the parameter space. Therefore, the horn solutions appear and disappear around the LSNP by saddle-node bifurcations. The smallest horn solution is stable inside the dashed zone represented in Fig. 11. This zone has been determined numerically for both the step and exponential influence functions. The other horn states have a similar region of stability inside the dashed zone and all these regions converge to a cusp point LSNP.

2. Localized pattern in the R_3 region

As a result of spontaneous breaking of spatial symmetry in this region, we observe front solutions connecting the unpopulated state with the periodic population one. These solutions are motionless for a large range of parameters. In order to study the localized structures in this region, one can consider the interaction of front pairs and obtain a similar expression to Eq. (14) amended with an extra periodic term [32]. The front interaction alternates between being attractive and repulsive. Hence, one can find an infinite number of localized structures, usually called *localized patterns* [32]. However, to obtain an analytical expression of the front interaction, one should be consider the system in the parameter region such that pattern and uniform states are nearby. Figures 12(c) and 12(d) show such localized patterns observed from model (2). These localized states are found above the solid line and inside the dotted curve. This curve in the R_3 region is the bifurcation separating the motionless fronts from propagating ones. The gray part in the R_3 region accounts for the pinning range.

Numerically, we have computed the region in which the shortest localized pattern—the localized state with fewest bumps—is stable. This region is represented in Fig. 11 by the zone enclosed by the dotted line and lying above the solid line $S(\alpha)$. Above this line and outside the dotted line, for small α, the periodical equilibrium state always invades the unpopulated one with a well-defined speed.

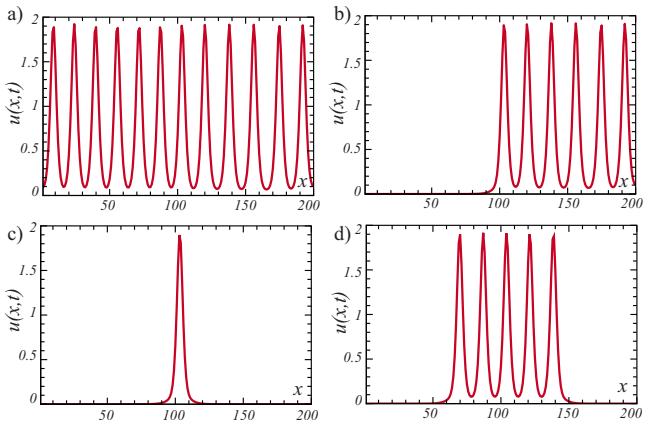

FIG. 12. (Color online) Pattern, front solution, and localized patterns observed from our model (2) for α=0.417, σ=2.7. (a) Periodic solution, (b) front solution that links the unpopulated state and the periodic fully populated state, (c) first bump localized pattern, and (d) eight-bump solutions.

It is important to note that, for the two influence functions that we have considered, the phase diagrams are qualitatively quite similar.

VI. RIVALRY OF COLONIES

The colonies under consideration represent particle-type solutions characterized and classified by their position and their width. They correspond to a self-organizing cluster. Considering two or more of theses colonies together, one might consider a conflict interaction between them as a consequence of finite resources. To study this competition, let us analyze the simple case of two shortest colonies (cf. inset of Fig. 13). With the help of the ansatz,

$$u = \zeta[x + \Delta(t)/2] + \zeta[x - \Delta(t)/2] + \phi_3(x,\Delta), \qquad (22)$$

where $\zeta(x-x_0)$ stands for the shortest colony solution, which is centered at position x_0, that is, maximum density of popu-

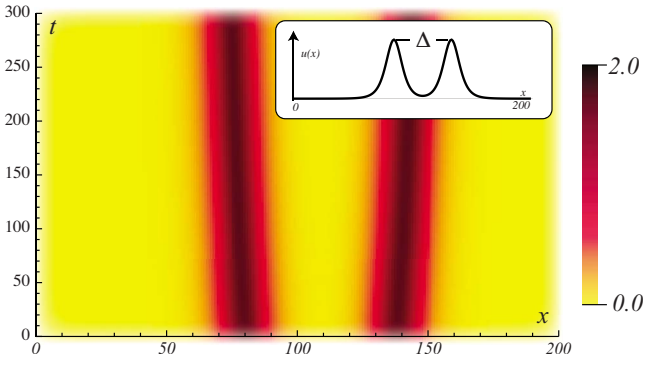

FIG. 13. (Color online) Spatiotemporal evolution of the population density $u(x,t)$ for model (2) for exponential influence function, α=0.59, σ=2.325, with time running up. The gray scale is proportional to the population density. The inset figure is the initial population density profile.

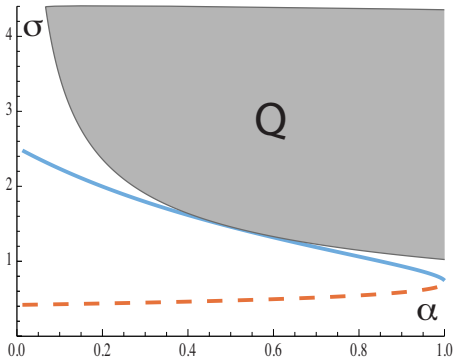

FIG. 14. (Color online) Bifurcation diagram of the variational nonlocal Nagumo model for the exponential influence function. In the Q region, the nonlocal interaction between localized structures is repulsive and dominates.

lation of the colony is located at x_0, Δ is the distance between colonies (cf. Fig. 13), and we assume initially that the colonies are remote $\Delta(t=0) \gg 1$. The interaction between theses structures occurs, again, by two mechanisms: (i) the exponential perturbation imposed by one colony on the other, which is order $e^{-\sqrt{\alpha}\Delta}$, and (ii) the nonlocal interaction given by the influence function. For a compact influence function the first mechanism dominates when the colonies are remote ($\Delta \gg 1$). On the other hand, for the exponential influence function the nonlocal interaction is long range and is of order $e^{-\Delta/\sigma}$. Thus, both mechanisms of interaction are exponential. In fact, in the region $Q=\{\sigma > 1/\sqrt{\alpha}\}$, the nonlocal interaction dominates. Figure 14 depicts the zone Q. It is easy to show that

$$S(\alpha) = \frac{\sqrt{2} + \sqrt{1-\alpha}}{(1+\alpha)} \leq 1/\sqrt{\alpha}.$$

The equality occurs only at the Maxwell point $\alpha_M = 1/2 (S(\alpha_M) = \sqrt{2})$, and the zone Q is then contained in the R_3 region. Hence, the firth order on the perturbation is $\phi_3 \sim \dot{\Delta} \sim e^{-\Delta/\sigma}$. Analogous to previous interaction calculations, we focus in a space region of one colony. For the sake of simplicity we consider around $-\Delta/2$, and introducing ansatz (22) in model (2) and linearizing in ϕ_3, we obtain

$$\mathcal{L}_\alpha[\zeta(x+\Delta/2)]\phi_3 = \frac{\dot{\Delta}}{2}\partial_x\zeta(x+\Delta/2) + \zeta(x+\Delta/2)\mathcal{N}\zeta^2(x-\Delta/2).$$

In order to solve the above equation, we have to impose the solvability condition

$$\dot{\Delta} = Ke^{-\Delta/\sigma}, \tag{23}$$

where

$$K = 2\frac{\int_{-\infty}^{\infty} e^{-z/\sigma}F(z)dz}{\sigma\int_{-\infty}^{\infty}(\partial_x\zeta)^2 dx}$$

and

$$F(z) = \int_{-\infty}^{\infty} \zeta(x)\partial_x\zeta(x)[\zeta^2(z-x) - \zeta^2(z+x)]dx.$$

$F(z)$ is an even function with the asymptotic form $F(z \sim \pm\infty) \sim e^{-2\sqrt{\alpha}|z|}$. Hence, the integral $\int e^{-z/\sigma}F(z)dz$ performed on the whole space converges. Note that, when the argument of the function F is positive (negative), the function is negative (positive). The above property is a consequence of $\zeta(x)$ that is a positive symmetric pulse-type function; then, $\partial_x\zeta(x)[\zeta^2(z-x) - \zeta^2(z+x)]$ is positive (negative) for z negative (positive). Hence, when $\int_{-\infty}^{\infty} e^{-z/\sigma}F(z)dz$ is positive, then K is also positive. Therefore, the interaction between colonies is repulsive. Figure 13 depicts the interaction between two shortest colonies in the spatiotemporal diagram obtaining numerically. From this picture we can deduce the interaction to be repulsive. The intensity of the interaction decreases with the distance between them. We conclude that there is quite a good agreement between the analytic and numerical results.

VII. CONCLUDING REMARKS

Succinctly stated, our work reported in the present papers has arisen from the interplay of two ingredients—Allee effect and spatially nonlocal competition interactions in the framework of reaction diffusion equations. The starting point we propose is integrodifferential model (2). Typically, integrodifferential equations are analytically inaccessible. However, on the basis of a well-characterized weakly nonlinear analysis, we have been able to understand thoroughly the dynamics exhibited by our model. We have characterized the bifurcation diagram for uniform states, pattern states, front solutions, and localized states. In particular, we have determined and characterized the critical-point in-phase space where the localized structures appear, the *localized structure nascent point*. The noteworthy feature of our analysis is that it is analytical and fully tractable.

One of the intriguing outcomes of our work here is that while, in the ecological context, colonies are commonly understood as arising from topographic conditions, we are able to propose a (and rather natural) mechanism for the appearance of colonies based on self-organization. The mechanism is a direct consequence of the Allee effect and spatially nonlocal competition. Depending on the initial conditions and parameter values, colonies and networks between then can develop by themselves.

Our theory and results should be of interest to a wide variety of phenomena, not only in ecological systems, in which the applications are obvious, but also in sociological systems involving informatics communication, infectious diseases, production, exchange, distribution, and consumption of goods and services, to mention only a few. Note also that in recent years great effort has been expended to understand vegetation dynamics, particularly the formation of patterns [12,33]. The processes of seed production, the dispersion and germination, or the interaction of biomass and soil water are modeled by nonlocal nonlinearity. In these

contexts, it is considered that the biomass is described by a nonlocal Fisher equation coupled with other variables. Replacement of the Fisher model by the nonlocal Nagumo model we propose might improve the understanding of the vast amount of localized states and patterns, such as "fairy circles" observed in the Namib desert [34]. Work in these directions is in progress.

ACKNOWLEDGMENTS

M.G.C. and D.E. acknowledge the support of FONDECYT Projects No. 1090045 and No. 11090280, respectively. V.M.K. acknowledges NSF support under Grant No. INT-0336343, DARPA support under Grant No. N00014-03-1-0900, and NIH/NSF support under Grant No. EF-0326757.

[1] J. D. Murray, *Mathematical Biology* (Springer-Verlag, Berlin, 1989).
[2] S. Camazine, J. L. Deneubourg, N. R. Franks, J. Sneyd, G. Theraulaz, and E. Bonabeau, *Self-Organization in Biological Systems* (Princeton University Press, Princeton, 2001).
[3] M. C. Cross and P. C. Hohenberg, Rev. Mod. Phys. **65**, 851 (1993).
[4] L. M. Pismen, *Patterns and Interfaces in Dissipative Dynamics*, Springer Series in Synergetics (Springer, Berlin, 2006).
[5] V. Mendez, S. Fedotov, and W. Horsthemke, *Reaction- Transport Systems: Mesoscopic Foundations, Fronts, and Spatial Instabilities* (Springer-Verlag, Berlin, 2010).
[6] M. A. Fuentes, M. N. Kuperman, and V. M. Kenkre, Phys. Rev. Lett. **91**, 158104 (2003).
[7] V. M. Kenkre, *Modern Challenges in Statistical Mechanics: Patterns, Noise, and the Interplay of Nonlinearity and Complexity*, AIP Conf. Proc. No. 658 (AIP, New York, 2003).
[8] M. A. Fuentes, M. N. Kuperman, and V. M. Kenkre, J. Phys. Chem. B **108**, 10505 (2004).
[9] E. Hernández-García and C. López, Phys. Rev. E **70**, 016216 (2004); C. López and E. Hernández-García, Physica D **199**, 223 (2004).
[10] D. G. Kendall, *Mathematics and Computer Science in Biology and Medicine* (H. M. Stationary Office, London, 1965).
[11] R. E. Goldstein, D. J. Muraki, and D. M. Petrich, Phys. Rev. E **53**, 3933 (1996).
[12] E. Gilad, J. von Hardenberg, A. Provenzale, M. Shachak, and E. Meron, Phys. Rev. Lett. **93**, 098105 (2004).
[13] V. Volpert and S. Petrovskii, Phys. Life. Rev. **6**, 267 (2009).
[14] M. G. Clerc, D. Escaff, and V. M. Kenkre, Phys. Rev. E **72**, 056217 (2005).
[15] D. Escaff, Int. J. Bifurcation Chaos **19**, 3509 (2009).
[16] D. A. Birch and W. R. Young, Theor Popul. Biol. **70**, 26 (2006).
[17] S. Pigolotti, C. Lopez, and E. Hernandez-Garcia, Phys. Rev. Lett. **98**, 258101 (2007).
[18] L. Gelens, D. Gomila, G. Van der Sande, M. A. Matias, and P. Colet, Phys. Rev. Lett. **104**, 154101 (2010).
[19] W. C. Allee, *Animal Aggregations: A Study in General Sociology* (University Chicago Press, Chicago, IL, 1931).
[20] W. C. Allee, *The Social Life of Animals* (Beacon Press, Boston, 1938).
[21] B. Perthame, *Transport Equations in Biology*, Frontiers in Mathematics (Springer-Verlag, New York, 2008).
[22] V. M. Kenkre and M. N. Kuperman, Phys. Rev. E **67**, 051921 (2003).
[23] M. N. Niraj Kumar, M. N. Kuperman, and V. M. Kenkre, Phys. Rev. E **79**, 041902 (2009).
[24] R. E. Goldstein, G. H. Gunaratne, L. Gil, and P. Coullet, Phys. Rev. A **43**, 6700 (1991).
[25] G. Iooss and M. Adelmeyer, *Topics in Bifurcation Theory and Applications* (World Scientific, Singapore, 1992).
[26] S. Residori, A. Petrossian, T. Nagaya, C. Riera, and M. G. Clerc, Physica D **199**, 149 (2004).
[27] P. Coullet, Int. J. Bifurcation Chaos **12**, 2445 (2002).
[28] C. Elphick, E. Tirapegui, M. Brachet, P. Coullet, and G. Iooss, Physica D **29**, 95 (1987).
[29] S. H. Strogatz, *Nonlinear Dynamics and Chaos* (Westview Press, Cambridge, 2000).
[30] Y. Pomeau, Physica D **23**, 3 (1986).
[31] M. G. Clerc, C. Falcon, and E. Tirapegui, Phys. Rev. Lett. **94**, 148302 (2005); Phys. Rev. E **74**, 011303 (2006).
[32] M. G. Clerc and C. Falcon, Physica A **356**, 48 (2005).
[33] R. Lefever, N. Barbier, P. Couteron, and O. Lejeune, J. Theor. Biol. **261**, 194 (2009).
[34] W. J. Jankowitz, M. W. Rooyen, D. Shaw, J. S. Kaumba, and N. V. Rooyen, S. Afr. J. Bot. **74**, 332 (2008).